

General solution to nonlinear optical quantum graphs using Dalgarno-Lewis summation techniques

Rick Lytel, Sean M. Mossman, and Mark G. Kuzyk

Department of Physics and Astronomy, Washington State University, Pullman, Washington 99164-2814

We develop an algorithm to apply the Dalgarno-Lewis (DL) perturbation theory to quantum graphs with multiple, connected edges. We use it to calculate the nonlinear optical hyperpolarizability tensors for graphs and show that it replicates the sum over states computations, but executes ten to fifty times faster. DL requires only knowledge of the ground state of the graph, eliminating the requirement to determine all possible degeneracies of a complex network. The algorithm is general and may be applied to any quantum graph.

I. INTRODUCTION

Quantum graphs were recently introduced as general models to explore the fundamental limits of nonlinear optics and to discover the topological and geometrical properties of structures that maximize the nonlinear optical response[1–5]. Like other Hamiltonian models, quantum graphs with specific shapes and topologies have nonlinear optical response near the fundamental limits[6].

A quantum graph is a metric graph on which electron dynamics is confined to the edges of the graph. Quantum graphs were first studied as tractable molecular models[7–11] and have been invoked as models of mesoscopic systems[12], optical waveguides [13], quantum wires[14, 15], excitations in fractals [16], and fullerenes, graphene, and carbon nanotubes[17–19]. Quantum graphs are also exactly solvable models of quantum chaos[20–23]. In nonlinear optics, quantum graphs are models of a branched nano-wire structure, or a quasi-linear molecule, such as a donor-acceptor, with side groups.

The solution of quantum graphs for nonlinear optics has used the sum over states perturbation theory developed decades ago[24]. The process requires determination of the eigenfunctions and energies of the graph for large numbers of states, and careful determination of the degenerate states comprising the spectrum. A Monte Carlo calculation of the response for a simple graph can take hours of computer time, frequent checks that the solutions for each graph are correct through the use of sum rules, and careful delineation of all degeneracies. The value of such simulations to the molecular designer has been investigated, and new design rules have been posited[25]. But the method does not scale well to graphs with many edges and large numbers of degenerate states that are often impossible to determine from a direct diagonalization of the Hamiltonian.

Recently, the Dalgarno-Lewis (DL) formulation of perturbation theory[26] has been adapted to off-resonance and dispersive nonlinear optics[27]. The DL approach requires knowledge of only the ground state of the structure. (For intrinsic nonlinearities[28], the ground and first excited state energies are also required.) As such,

it offers a huge computational advantage for large-scale calculations, as only a single eigenfunction must be specified. Degeneracies are implicitly incorporated into the DL formulation. Application of the DL formalism to quantum graphs opens up the possibility of a general computational approach for exploring the theory of fundamental limits, as well as for simulating molecular and nanostructures that might achieve larger intrinsic nonlinear optical responses.

Section II reviews the solution of quantum graphs and the use of the sum over states to compute the nonlinearities. Section III introduce the DL formalism and formally adapts it directly to quantum graphs. Section IV develops the general algorithm for solving quantum graphs using the results of Section III and illustrates it with wire, star, loop, and a composite, seven-edged graph, and displays the accuracy and computational speedup of the method over the sum over states. Section V summarizes the benefits of the method and its extension to dispersive nonlinear optics.

II. COMPUTATION WITH QUANTUM GRAPHS

Optimization studies using quantum graphs are based upon Monte Carlo computations with tens to hundreds of thousands of possible geometries for a particular topology, such as a star or loop motif[29], or a composite of stars, loops, and wires. For each structure, the Hamiltonian is diagonalized to find the energy spectrum E_n and the eigenstates $|n\rangle$, where n is the mode number. The transition moments $r_{nm}^i = \langle n|r^i|m\rangle$ are computed for the graph using a union operation[2], and the first and second hyperpolarizability tensors β_{ijk} and γ_{ijkl} are calculated using perturbation theory based upon the sum over states[24]:

$$\beta_{ijk} = \left(\frac{e^3}{2}\right) P_{ijk} \sum_{nm} \frac{r_{0n}^i \bar{r}_{nm}^j r_{m0}^k}{E_{n0} E_{m0}} \quad (1)$$

and

$$\gamma_{ijkl} = \left(\frac{e^4}{6}\right) P_{ijkl} \left(\sum_{nmp} \frac{r_{0n}^i \bar{r}_{nm}^j \bar{r}_{mp}^k r_{p0}^l}{E_{n0} E_{m0} E_{p0}} - \sum_{nm} \frac{r_{0n}^i r_{n0}^j r_{0m}^k r_{m0}^l}{E_{n0} E_{n0} E_{m0}} \right) \quad (2)$$

where $\bar{r}_{nm}^i = r_{nm}^i - \delta_{nm} r_{00}^i$, $E_{n0} = E_n - E_0$, and the permutation operator P permutes all indices into all possible permutations without regard to order. The indices are $i = x, y$ for a planar graph embedded in two-dimensional space. Both hyperpolarizabilities have been normalized to their maximum values[28] and are bounded above by unity. The lower bound on $|\beta_{ijk}|$ is zero, while that for γ_{ijkl} is -0.25 . The geometry of the structure largely determines the total contributions of the transition moments from each edge, each of which is determined by the mode overlap of the eigenfunctions with the appropriate position operator and the relative orientation of the edges. Tailoring this overlap and the change in the dipole moment for electron excitation from the ground state to an excited state can lead to a giant enhancement of the nonlinear optical response due to phase disruption of the eigenfunctions $\psi_n(s) = \langle s|n\rangle$, where s is measured along the graph[25].

Figure 1 illustrates the notation for computation with quantum graphs. Each edge has a coordinate s_p measured along the edge from zero to a_p and an angle θ_p with respect to an external axis, which we choose to be the x -axis for convenience. The edge functions $\phi_n^{(p)}(s_p)$ for edge p and mode n on that edge satisfy $H\phi_n^{(p)} = E_n\phi_n^{(p)}$, where the energies E_n are the same on all p edges. The full eigenfunctions ψ_n are constructed using a mathematical union operation

$$\psi_n(s) = \bigcup_{p=1}^E \phi_n^{(p)}(s_p) \quad (3)$$

operating on all E edges[2]. The Hilbert space for the solutions to the entire graph is a direct sum of those for each individual edge. The interpretation of the coordinates in Eqn 3 is that when the electron is on edge p , the eigenfunction $\psi_n(s)$ is equal to $\phi_n^{(p)}(s)$ for any mode n .

The construction of the union of edge functions to make an eigenfunction of the graph requires matching of boundary conditions at the vertices within the graph. For quantum graph unions, the boundary conditions are that the edge functions at each vertex are equal, and that the net probability flux into or out of a vertex is zero, or equivalently

$$\sum_p \frac{d\phi_n^{(p)}(s_p)}{ds_p} \Big|_v = 0 \quad (4)$$

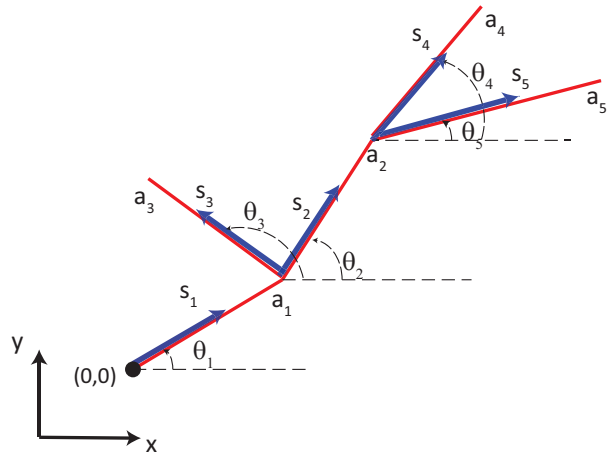


FIG. 1. A five-edge quantum graph, with two 3-star motifs, defining the coordinates and geometry used in the text.

where the sum is over the E_v edges going into or out of the vertex v . There are always enough boundary conditions to compute all of the constants of integration from the solutions of the edge functions.

The transition moments are computed by projecting the coordinate vector s_i for a given edge i onto the x -axis to compute $\langle n|x^i|m\rangle = \langle n|s_i|m\rangle \cos\theta_i$ and onto the y -axis to compute $\langle n|y^i|m\rangle = \langle n|s_i|m\rangle \sin\theta_i$ for each edge. Projected into coordinate space, the transition moments take the form of sums of definite integrals. For example, for x_{nm} , we get

$$x_{nm} = \sum_{p=1}^E \cos\theta_p \int_0^{a_p} ds_p s_p \phi_n^{(p)}(s_p) \phi_m^{(p)}(s_p) \quad (5)$$

where the sum is over the E edges, with a similar expression with $\cos \rightarrow \sin$ for y_{nm} . The solution of a quantum graph yields the spectrum and transition moments required by Eqns 1 and 2 for the hyperpolarizability tensors. Once a graph is specified by its metric variables a_p, θ_p and the potentials acting on each edge, the dependence of the magnitudes of the hyperpolarizabilities on the geometry and topology of the graph is computable and may be studied using Cartesian or spherical tensor analysis[2, 30].

Explorations of the topological structures maximizing the hyperpolarizabilities require computation of β_{ijk} and γ_{ijkl} for each of tens of thousands of graphs. Computation for each graph requires solving the graph for its energies and eigenfunctions, typically for at least 10–50 modes, depending on the nature of the potential energy. A single Monte Carlo run for a simple three-edged graph might require several hours of execution time on an eight-threaded, quad-core Intel *i7* CPU clocked at 3.7GHz. The computation requires careful handling of the solu-

tions of the graph to ensure that any and all degenerate states are discovered and enumerated. For a typical computation, it is necessary to invoke the Thomas-Reiche-Kuhn (TRK) sum rules[31–33] to ensure that all such states have been correctly captured and the spectra correctly determined[2]. Computation of a quantum graph for nonlinear optics is an elaborate procedure that is time-consuming and often frustrating when graph geometries produce numerous degeneracies. The Dalgarno-Lewis perturbation theory offers a simplification of the Monte Carlo computation and an execution time speedup of over a factor of 50.

III. DALGARNO-LEWIS PERTURBATION THEORY

The Dalgarno-Lewis perturbation method has been reviewed in the literature[26, 34–36] and in classic quantum mechanics textbooks[37]. A paper in the present volume describes its application to dispersive nonlinear optics and solves a number of one-dimensional examples. Quantum graphs are quasi-one dimensional objects, with particle motion along the edges of the graph and not transverse to it. But they live in two dimensions and have x and y projections that contribute to the hyperpolarizability tensors. Moreover, their Hilbert space is a direct sum of Hilbert spaces for each of the edges, which adds complexity to the DL formalism and for which no algorithms have yet been developed. This section summarizes the DL formalism for one dimension and then extends it to quantum graphs for the first time.

A. DL theory in one dimension

The Dalgarno-Lewis method for perturbation theory in one dimension begins by assuming the existence of an operator F whose commutator with the Hamiltonian $H = p^2/2m + V$ takes the form

$$[F, H] = \bar{x} \quad (6)$$

with $\bar{x} = x - x_{00}$. The right-hand side is essentially the perturbing potential on a molecule in an electric field, $V = -ex$, with the ground state expectation value subtracted and the electric charge e dropped, as it will be incorporated elsewhere later.

Acting on the ground state with both sides of Eqn 7 yields

$$[F, H] |0\rangle = \bar{x}|0\rangle \quad (7)$$

If we operate on the left of both sides of Eqn 7 with $\langle n|$ and use $H|n\rangle = E_n|n\rangle$, we get

$$F_{n0} = -\frac{\bar{x}_{n0}}{E_{n0}} \quad (8)$$

which defines matrix elements of the F operator in a way that allows a substitution into the sum over states expressions for β_{xxx} :

$$\begin{aligned} \beta_{xxx} &= 3e^3 \sum'_{n,m} \frac{x_{0n} \bar{x}_{nm} x_{m0}}{E_{n0} E_{m0}} \quad (9) \\ &= -3e^3 \sum'_{n,m} F_{0n} \bar{x}_{nm} F_{m0} \\ &= -3e^3 \langle 0|F\bar{x}F|0\rangle \end{aligned}$$

where the last line in Eqn 9 follows by using completeness of the eigenstates. If the DL operator exists, then the first hyperpolarizability is computable through the ground state expectation value of the composite operator $F\bar{x}F$. Evidently, the effect of the perturbation on the excited states and their contributions to β_{xxx} are embodied in the F operator.

To obtain a spatial representation for F that we may use in computations, we project Eqn 7 into coordinate space as follows. The Hamiltonian, in coordinate space, is given by

$$H = -\frac{\hbar^2}{2m} \frac{d^2}{dx^2} + V(x), \quad (10)$$

We want to project Eqn 6 into position space, where we know $\langle x|0\rangle = \psi_0(x)$ is the ground state wavefunction. We will need the projection of F into x -space, which is defined through

$$\langle x|F|0\rangle = \int dx' \langle x|F|x'\rangle \langle x'|0\rangle \quad (11)$$

$$= F(x)\psi_0(x) \quad (12)$$

which defines the function $F(x)$. We are asserting that $F(x)$ exists for our operator. If we can derive an expression for it, then we will have found a representation for the F operator and may use Eqn 9 to compute the first hyperpolarizability as an expectation value of $F\bar{x}F$ in the *unperturbed* ground state. Note that we do not even need to know the spectrum. The energy scale won't enter into the problem until we divide by β_{max} from the theory of fundamental limits. We'll return to this later.

Projecting the left-hand side (LHS) of Eqn 7 into x -coordinate space gives

$$\begin{aligned} LHS &= F(x) \left(-\frac{\hbar^2}{2m} \frac{d^2}{dx^2} + V(x) \right) \psi_0(x) \quad (13) \\ &\quad - \left(-\frac{\hbar^2}{2m} \frac{d^2}{dx^2} + V(x) \right) F(x)\psi_0(x) \\ &= \frac{\hbar^2}{2m} \left(\frac{d^2 F(x)}{dx^2} \psi_0(x) + 2 \frac{dF(x)}{dx} \frac{d\psi_0(x)}{dx} \right) \\ &= \frac{\hbar^2}{2m} \frac{1}{\psi_0(x)} \frac{d}{dx} \left((\psi_0(x))^2 \frac{dF(x)}{dx} \right). \end{aligned}$$

Projecting the right-hand side of Eqn 7 into coordinate space yields

$$RHS = \bar{x}\psi_0(x) \quad (14)$$

Equating Eqns 13, and 14, we get the differential equation

$$\frac{d}{dx} \left((\psi_0(x))^2 \frac{dF(x)}{dx} \right) = \frac{2m}{\hbar^2} \bar{x} (\psi_0(x))^2. \quad (15)$$

The general solution to Eqn 15 is obtained with two quadratures:

$$F(x) = F(0) + \frac{2m}{\hbar^2} \int_0^x \frac{dx'}{\psi_0(x')^2} \quad (16)$$

$$\times \left(\int_0^{x'} dx'' \bar{x}'' \psi_0(x'')^2 + \frac{\hbar^2}{2m} F'(0) \psi_0(0)^2 \right)$$

Eqn 16 is the main result. Note that the lower limit of the inner integral could have been chosen to be some value δ , where $F'(\delta)\psi_0(\delta)^2 = 0$, but we choose $\delta = 0$ for quantum graphs. Once the ground state wavefunction is known, the function $F(x)$ may be found by analytical or numerical integration, once two boundary conditions are specified. Actually, for bounded problems, such as a quantum well where the wavefunction vanishes at each end, the second term in Eqn 16 vanishes without specifying a boundary condition $F'(0)$. We may always choose $F(0)$ any way we please, because the operator F is determined by a commutator and is therefore only known up to a constant anyway.

To calculate γ from the sum over states, we need an additional operator G . In analogy with Eqn 7, we intuit that this is

$$[G, H] |0\rangle = [\bar{x}F - \langle 0|\bar{x}F|0\rangle] |0\rangle \quad (17)$$

which leads to a differential equation for $G(x)$, the projection of G into coordinate space. The solution to this equation may be written down by inspection of Eqn 16 and is

$$G(x) = G(0) \quad (18)$$

$$+ \frac{2m}{\hbar^2} \int_0^x \frac{dx'}{\psi_0(x')^2} \left(\int_0^{x'} dx'' [\bar{x}'' F(x'') - \langle 0|\bar{x}'' F|0\rangle] \psi_0(x'')^2 + \frac{\hbar^2}{2m} G'(0) \psi_0(0)^2 \right).$$

Eqn 17 implies that

$$G_{n0} = -\frac{\langle \bar{x}F \rangle_{n0}}{E_{n0}} \quad (19)$$

which may be used to write Eqn 2 in a compact sum of ground state expectation values of operator products of the form $F^p x^q G^r$ with integers p, q, r . We present an explicit form in the next section that is applicable to quantum graphs.

Note that we have defined the action of the anti-Hermitian operator F on the ground state $F|0\rangle$ to be

equal in x-space to $F(x)\psi_0(x)$. This implies that the adjoint has a minus sign: $\langle 0|F$ becomes $-F^*(x)\psi_0^*(x)$. This is important because operator products like FF will produce minus signs when they are sandwiched between ground states. The same is true for G if it acts to the left.

B. Extension to quantum graphs

We can easily extend the one dimensional Dalgarno-Lewis formalism to quasi-one dimensional graphs using the fact that the Hamiltonian rotates as a quadratic form, viz., $H(x, y) \rightarrow H(s) + H(\tau)$ and ignoring the transverse part[38]. This implies that all of our one-dimensional work carries through for the F and G functions, except now the coordinates on the right hand side of Eqn 7 and 17 are either x or y , depending on the transition moment one wishes to calculate. With this in mind, we arrive at

$$F_i(s) = F_i(0) + \frac{2m}{\hbar^2} \int_0^s \frac{ds'}{\psi_0(s')^2} \quad (20)$$

$$\times \left(\int_0^{s'} \bar{r}^i(s'') \psi_0(s'')^2 ds'' + \frac{\hbar^2}{2m} F_i'(0) \psi_0(0)^2 \right)$$

where $r^1 = x$ and $r^2 = y$. The coordinate variable s is measured along the graph edges. The wavefunction and DL functions in Eqn 20 are unions of functions defined on the graph edges. The interpretation of the integral is that when s is on edge p , the values of the edge functions on edge p are to be used, and the coordinate variable spans the range of that edge function. We quantify this description in Section IV.

For γ , we use the new set of functions, G_{ij} defined by the commutator $[G_{ij}, H] = \bar{r}^i F_j - \langle 0|\bar{r}^i F_j|0\rangle$, which translates in s-space to an equation for $G_{ij}(s)$ which is identical to that for F_i in Eqn 20, but with an inner integrand given by the product $\bar{r}^i F_j - \langle 0|\bar{r}^i F_j|0\rangle$ expressed in s-space. The explicit form is

$$G_{ij}(s) = G_{ij}(0) = \frac{2m}{\hbar^2} \int_0^s \frac{ds'}{\psi_0(s')^2} \quad (21)$$

$$\times \left(\int_0^{s'} [\bar{r}^i(s'') F_j(s'') - \langle 0|\bar{r}^i F_j|0\rangle] \psi_0(s'')^2 ds'' + \frac{\hbar^2}{2m} G_{ij}'(0) \psi_0(0)^2 \right).$$

Note that the s variable appearing in each of Eqns 20 and 21 roams over the entire graph and that $\psi_0(s)$ is the ground state wavefunction for the graph, which is the union of the edge functions.

It is now straightforward to derive simple expressions for the hyperpolarizabilities. First, we note that it is always possible to add a constant to F to make $\langle 0|F|0\rangle =$

0 so we will assume that has always been done. Eqn 8 then allows us to write the expression for β_{ijk} in Eqn 1 without energy denominators as

$$\beta_{ijk} = -P_{ijk} \left(\frac{e^3}{2} \right) \left(\langle 0|F_i r^j F_k|0\rangle - r_{00}^j \langle 0|F_i F_k|0\rangle \right). \quad (22)$$

We note that we can also add a constant to G to make $\langle 0|G|0\rangle = 0$ without changing the commutator that defined G. We will always assume we have done this. Given this, we may use Eqn 19 to write down the general expressions for $\gamma_{ijkl} = \gamma_{ijkl}^{(1)} - \gamma_{ijkl}^{(2)}$ as

$$\begin{aligned} \gamma_{ijkl}^{(1)} &= P_{ijkl} \left(\frac{e^4}{6} \right) \langle 0|F_i \bar{r}^j G_{kl}|0\rangle \\ \gamma_{ijkl}^{(2)} &= P_{ijkl} \left(\frac{e^4}{6} \right) \langle 0|F_i F_j|0\rangle \langle 0|r^k F_l|0\rangle \end{aligned} \quad (23)$$

This completes the *formal* specification of the F and G functions, and their use in calculating the hyperpolarizabilities. To apply this formalism to quantum graphs, we must express the DL functions in the language of the direct sum Hilbert space they represent.

IV. GENERAL SOLUTION FOR QUANTUM GRAPHS.

For graphs, the meaning of eigenfunctions $\psi_n(s)$ and ground state expectation values require sharp definition of the union operation that stitches together the Hilbert spaces on each edge to yield a direct sum Hilbert space with energies equal to those of the spaces for each edge. Continuity and flux conservation, Eqn 4, showed how this is accomplished for the edge functions. With this algorithm, Eqn 5 showed how expectation values of operators acting across a graph are calculated, edge by edge, for transition moments. For F_i and G_{ij} , we need the union of an F or G function tied to each edge:

$$F_i(s) = \bigcup_{p=1}^E F_i^{(p)}(s_p) \quad (24)$$

with a similar union operation defined for G_{ij} :

$$G_{ij}(s) = \bigcup_{p=1}^E G_{ij}^{(p)}(s_p). \quad (25)$$

Here and going forward, the index i refers to the Cartesian component x or y of an object, while the index p refers to a mode number.

The matching of the edge $F_i^{(p)}$ and $G_{ij}^{(p)}$ functions at vertices is accomplished by demanding continuity of each at the vertex and a net flow into or out of the vertex equal to zero. A ground state expectation value of the form of

Eqn 5 (with $m=n=0$) but for $x F_x$, say, would then be calculated as

$$\langle 0|x F_x|0\rangle = \sum_{p=1}^E \cos \theta_p \int_0^{a_p} ds_p s_p F_x^{(p)}(s_p) \phi_0^{(p)}(s_p) \phi_0^{(p)}(s_p) \quad (26)$$

with a similar expression for expectation values of other products of operators. The boundary conditions arising from the union operation completely specify all integration constants appearing in the edge DL functions and provide a general solution to the problem of calculating the first and second hyperpolarizabilities from only expectation values of products of DL operators. For clarity, going forward, *we drop the mode subscript 0 on the edge functions in the ground state by writing $\phi_0^{(p)}(s_p) \equiv \phi^{(p)}(s_p)$.*

The explicit forms of the $F_i^{(p)}$ and $G_{ij}^{(p)}$ DL edge functions are

$$\begin{aligned} F_i^{(p)}(s_p) &= F_i^{(p)}(0) + \frac{2m}{\hbar^2} \int_0^{s_p} \frac{ds'_p}{\phi^{(p)}(s'_p)^2} \\ &\times \left(\int_0^{s'_p} \bar{r}^i(s''_p) \phi^{(p)}(s''_p)^2 ds''_p + \frac{\hbar^2}{2m} F_i^{(p)}(0) \phi^{(p)}(0)^2 \right) \end{aligned} \quad (27)$$

and

$$\begin{aligned} G_{ij}^{(p)}(s_p) &= G_{ij}^{(p)}(0) = \frac{2m}{\hbar^2} \int_0^{s_p} \frac{ds'_p}{\phi^{(p)}(s'_p)^2} \\ &\times \left(\int_0^{s'_p} [\bar{r}^i(s''_p) F_j^{(p)}(s''_p) - \langle 0|\bar{r}^i F_j|0\rangle] \phi^{(p)}(s''_p)^2 ds''_p \right. \\ &\left. + \frac{\hbar^2}{2m} G_{ij}^{(p)}(0) \phi^{(p)}(0)^2 \right). \end{aligned} \quad (28)$$

where the angular brackets signify the expectation value in the ground state DL edge function. The integration constants are selected to satisfy the boundary conditions on the DL functions so their union is a function that is the projection of the DL operator F or G into coordinate space over the entire graph. The boundary conditions are that the $F_i^{(p)}(s_p)$ are equal at the vertex where the edges which they are index meet, and the sum of the derivatives with respect to their edge coordinates, measured into or out of a vertex, of all edges meeting at that vertex vanishes. Similar conditions hold for $G_{ij}^{(p)}$ and its derivatives.

The first integral of the DL equation for $F_i^{(p)}(s_p)$ for any edge p of a graph may be written as

$$F_x^{(p)}(s_p) \phi^{(p)}(s_p)^2 = F_x^{(p)}(0) \phi^{(p)}(0)^2 + \frac{2m}{\hbar^2} \int_0^{s_p} ds'_p \bar{x}(s'_p) \phi^{(p)}(s'_p)^2 \quad (29)$$

where $\bar{x}(s'_p) = x_{0p} + \cos \theta_p s'_p - x_{00}$ for the i th edge. Here, x_{0p} is the offset from the origin for edge p , and $F' = d/ds$. In particular, the following relationship holds at

the endpoints of an edge:

$$\begin{aligned} & F_x^{(p)}(a_p)\phi^p(a_p)^2 - F_x^{(p)}(0)\phi^{(p)}(0)^2 \quad (30) \\ &= \frac{2m}{\hbar^2} \int_0^{a_p} ds'_p \bar{x}(s'_p) \phi^{(p)}(s'_p)^2 \\ &\equiv \frac{2m}{\hbar^2} \langle \bar{x}_p \rangle \end{aligned}$$

Note that each DL function for edge p has two integration constants. We show how the boundary conditions determine these constants. Write Eqn 27 as

$$\begin{aligned} F_x^{(p)}(s_p) &= F_x^{(p)}(0) + \frac{2me}{\hbar^2} \int_0^{s_p} \frac{ds'_p}{\phi^{(p)}(s'_p)^2} \quad (31) \\ &\times \left(\int_0^{s'_p} ds''_p \bar{x}(s''_p) \phi^{(p)}(s''_p) + C_p \right) \end{aligned}$$

where the first integration constants are

$$C_p = \frac{\hbar^2}{2m} F_x^{(p)}(0) \phi^p(0)^2 \quad (32)$$

and are proportional to the net flux entering edge p . Now write Eqn 30 as

$$F_x^{(p)}(a_p) \phi^p(a_p)^2 = \frac{2m}{\hbar^2} [C_p + \langle \bar{x}_p \rangle] \quad (33)$$

which is proportional to the net flux exiting edge p times the square of the p th edge function evaluated at the exit vertex. Eqns 32 and 33 reveal that two edges $p1$ and $p2$ have a common vertex, say at $a_{p1} = a_{p2} = 0$, then the C_{p1} and C_{p2} for edges $p1$ and $p2$ are related by flux conservation. Eqns 32 and 33 may thus be used to conserve DL function flux at each vertex. A final set of equations matches the values of the DL functions at each vertex:

$$F_x^{(E_1)}(v; 1) = F_x^{(E_2)}(v; 2) = \dots F_x^{(E_d)}(v; d) \quad (34)$$

for every set of d edges that come together at vertex v , and the notation $(v; n)$ means evaluate at the position s_n for that edge at vertex v .

The continuity of $F_x^{(p)}$ and conservation of $F_x^{(p)}$ resemble the boundary conditions on the edge functions in a quantum graph. These embody the definition of a union of functions operating on the edges.

For the G functions, a similar approach applies, with Eqn 28 replaced by

$$\begin{aligned} G_{xx}^{(p)}(s_p) &= G_{xx}^{(p)}(0) + \frac{2m}{\hbar^2} \int_0^{s_p} \frac{ds'_p}{\phi^{(p)}(s'_p)^2} \quad (35) \\ &\times \left(\int_0^{s'_p} ds''_p \left[\bar{x}(s''_p) F_x^{(p)}(s''_p) - \langle 0 | \bar{x} F_x | 0 \rangle \right] \phi^{(p)}(s''_p)^2 \right. \\ &\left. + D_p \right) \end{aligned}$$

for the xx component, with suitable modifications made for the yy and off-diagonal components. The constants D_p are proportional to the $G_{xx}^{(p)}$ flux entering edge p .

$$D_p = \frac{\hbar^2}{2m} G_{xx}^{(p)}(0) \phi^p(0)^2 \quad (36)$$

where this latter derivative may be obtained from an expression similar to Eqn 30, viz.,

$$\begin{aligned} & G_{xx}^{(p)}(a_p) \phi^p(a_p)^2 - G_{xx}^{(p)}(0) \phi^{(p)}(0)^2 \quad (37) \\ &= \frac{2m}{\hbar^2} \int_0^{a_p} ds'_p \left[\bar{x}_p(s'_p) F_x^{(p)}(s'_p) - \langle 0 | \bar{x} F_x | 0 \rangle \right] \phi^{(p)}(s'_p)^2 \\ &\equiv \frac{2m}{\hbar^2} \langle [\bar{x}_p F_x^{(p)} - \langle 0 | \bar{x} F_x | 0 \rangle] \rangle \end{aligned}$$

leading to

$$G_{xx}^{(p)}(a_p) \phi^{(p)}(a_p)^2 = \frac{2m}{\hbar^2} \left[D_p + \langle [\bar{x}_p F_x^{(p)} - \langle 0 | \bar{x} F_x | 0 \rangle] \rangle \right] \quad (38)$$

where again the brackets on the last term are the ground state expectation value in edge p .

Eqns 36 and 38 may be used to conserve DL function flux at each vertex. A final set of equations matches the values of the DL functions at each vertex:

$$G_{xx}^{(E_1)}(v; 1) = G_{xx}^{(E_2)}(v; 2) = \dots G_{xx}^{(E_d)}(v; d) \quad (39)$$

for every set of d edges that come together at vertex v , where again the notation $(v; n)$ means evaluate at the position s_n for that edge at vertex v .

The method derived in this section is applicable to any quantum graph. It is easy to use and will be illustrated with examples of wires, stars, and loops, and then applied to solve a seven-edge graph with three stars. This graph may have numerous degeneracies, depending on the relative edge lengths, that are challenging to discover[4, 5]. With the DL method, the solutions may be written down by inspection and easily coded, requiring only the ground state of the graph. This is an enormous simplification in solving the graph and leads to reduction in execution time for a large scale Monte-Carlo calculation from several hours to several minutes.

In the following examples, we consider $i = x$ for clarity. A similar set of results applies for the y direction by replacing x with y in the inner integrals' transition moment on each edge. *We suppress the x -index to simplify notation.*

A. Wire graphs.

Consider a three wire graph, as shown in the left panel of Figure 2. We need to solve for the $F_x^{(p)}$ (and $F_y^{(p)}$) on each edge so that we may compute matrix elements of

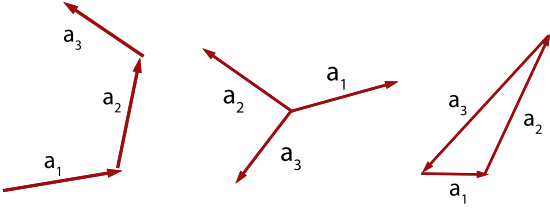


FIG. 2. Three wire (left), 3-star (center), and loop (right) graphs used to illustrate how to compute the F functions for the edges.

the union over edges of $F_x = \bigcup_p F_x^{(p)}$ (and $F_y = \bigcup_p F_y^{(p)}$) in the ground state.

Examining the graph and Eqn 32, it is easy to see that $C_1 = 0$ because the edge function $\phi^{(1)}(0) = 0$. To calculate C_2 , we note that it is just the flux entering edge 2, which is also the flux exiting edge 1, and by Eqn 33, we get $C_2 = C_1 + \langle \bar{x}_1 \rangle$, so $C_2 = \langle \bar{x}_1 \rangle$. Continuing, the flux entering edge three is C_3 is the flux exiting edge 2, which by Eqn 33 is $C_2 + \langle \bar{x}_2 \rangle$, so $C_3 = \langle \bar{x}_1 \rangle + \langle \bar{x}_2 \rangle$. Summarizing,

$$\begin{aligned} C_1 &= 0 \\ C_2 &= \langle \bar{x}_1 \rangle \\ C_3 &= \langle \bar{x}_1 \rangle + \langle \bar{x}_2 \rangle \\ &= -\langle \bar{x}_3 \rangle \end{aligned} \quad (40)$$

where the last equality in Eqn 40 follows from the fact that summing over all edges E,

$$\sum_{p=1}^E \langle \bar{x}_p \rangle = \sum_{p=1}^E \langle x_p \rangle - x_{00} = 0 \quad (41)$$

by definition of x_{00} .

Eqn 44 then requires that

$$\begin{aligned} F_1(a_1) &= F_2(0) \\ F_2(a_2) &= F_3(0) \end{aligned} \quad (42)$$

It is straightforward to arrange these conditions once the Fs are computed from Eqns 27, 32, and 33. Note that this leaves one overall undetermined constant, $F_1(0)$. We can always choose this constant such that the unions of the edge DL functions have zero ground state expectation value, $\langle 0|F|0 \rangle = 0$. The Gs are computed in the same way using 28, 36, and 38. This allows us to use the simple expressions for the hyperpolarizabilities displayed in Eqns 22 and 23.

B. Star graphs

Consider next a 3-star graph, as shown in the center panel of Figure 2. If we write the three edges in the

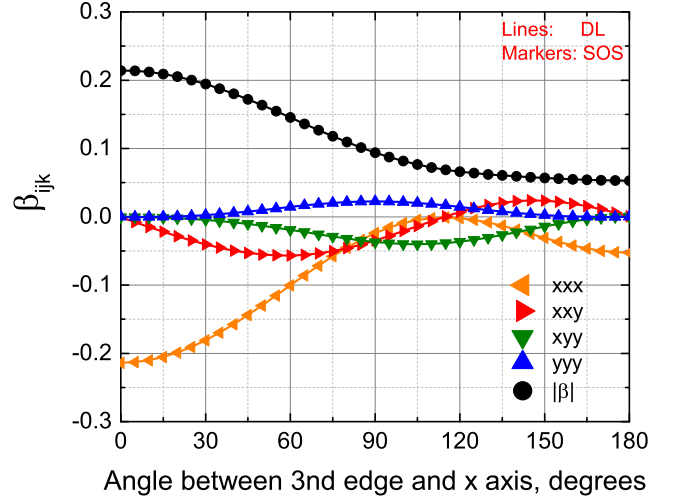


FIG. 3. Comparison of the Dalgarno-Lewis results for β_{ijk} for the 3-star graph with those obtained using the full SOS for all tensor components. In the legend, $xxx \equiv \beta_{xxx}$, etc.

canonical form of Eqn 27 and measure distance from the center vertex, we find from Eqn 32 and Eqn 33 that $C_1 = -\langle \bar{x}_1 \rangle$, $C_2 = -\langle \bar{x}_2 \rangle$, and $C_3 = -\langle \bar{x}_3 \rangle$ which is also equal to $\langle \bar{x}_1 \rangle + \langle \bar{x}_2 \rangle$ by Eqn 41. All of the $F_x^{(p)}$ are equal at the central vertex, and this is automatically satisfied if each of the F constants in Eqn 20 are equal. The value of this single constant may be set by demanding $\langle 0|F|0 \rangle = 0$, as noted above.

Figure 3 shows the results of using DL to calculate all of the tensor components of β_{ijk} for a 3-star graph with two fixed edges of lengths 0.4 and 0.2, angles of 180 and 90 degrees relative to the x-axis, and one rotating edge of fixed length $a_3 = 0.6$, and compares them to those calculated by using the sum over states with thirty modes. The DL method works with high precision. Figure 4 shows the calculations for γ_{ijkl} . Note that the length scale is arbitrary, as these are intrinsic hyperpolarizabilities; the relative lengths determine the response of the structure.

The most remarkable thing about using DL for these sets of star graphs is that states (4,5), (10,11), etc. are degenerate in energy (where $n = 0$ is the ground state), and the sum over states calculation requires identification of these states and diagonalization of the degenerate subspaces before it may be used. The DL computations don't know about any of this—they just require the (nodeless) ground state wavefunction. The DL operators, which implicitly sum up all of the contributions in perturbation theory from the excited states, automatically account for the degeneracies, as they followed from completeness of the unperturbed eigenstates.

The second remarkable feature of the DL summation technique is illustrated in Figure 5, which shows the massive speedup of DL over the sum over states with large

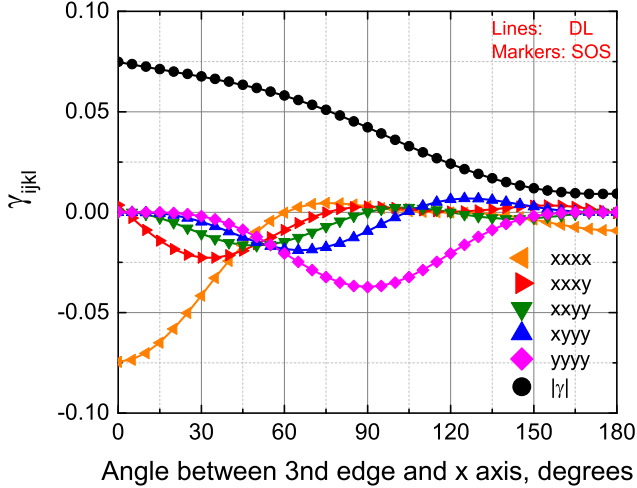


FIG. 4. Comparison of the Dalgarno-Lewis results for γ_{ijkl} for the 3-star graph with those obtained using the full SOS for all tensor components. In the legend, $xxxxx \equiv \gamma_{xxxxx}$, etc.

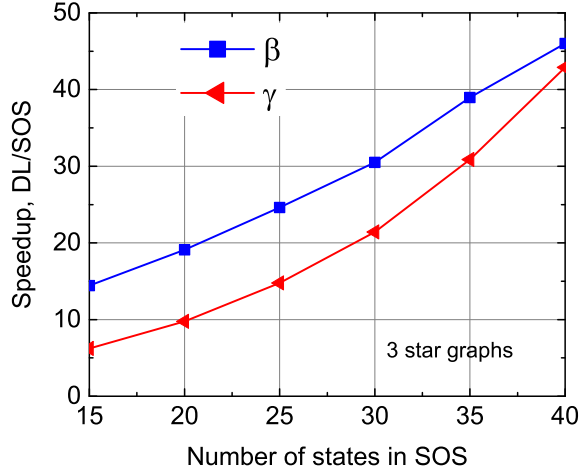


FIG. 5. Speedup of Dalgarno-Lewis computations over the sum over states.

numbers of modes.

C. Loops

Figure 2, right, shows a three-sided, closed loop graph. The computation of β_{ijk} and γ_{ijkl} for this class of graphs has been extensively discussed[1]. The ground state is nondegenerate, and is a constant, with zero energy. The excited state spectrum is doubly-degenerate. The eigenvalues are $k_n = 2\pi n/L$, where L is the perimeter of the loop.

The computation of the hyperpolarizabilities using DL may be accomplished by using Eqn 27 but with a single edge and sequential calculation[39]. For the x direction,

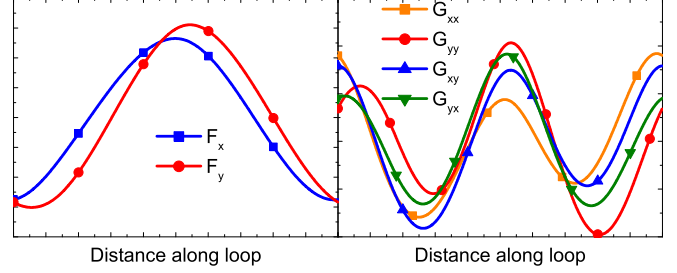


FIG. 6. Plots of the F_i and G_{ij} functions for the closed loop graphs, showing their periodicity, as expected. Numerical values on the y axis have been suppressed for clarity.

say, we get

$$F(s) = F(0) + \frac{2m}{\hbar^2} \int_0^s \frac{ds'}{\phi(s')^2} \times \left(\int_0^{s'} ds'' \bar{x}(s'') \phi(s'')^2 + C \right) \quad (43)$$

with a similar equation for the y component of F. For a continuous wire graph, including a loop, we may use the sequential edge method of calculation[39], where we measure distance s along the graph from an arbitrary starting point and change the value of $\bar{x}(s)$ in Eqn 43 when we move from one edge to the next. In this way, we can solve for the F and G functions for this graph by using Eqn 43 and an equivalent one for G by selecting the correct boundary conditions.

For a loop graph, we demand that $F(L) = F(0)$, in order to make F periodic as the particle circulates the graph. From Eqn 43, this requires that the first integration constant C be chosen so that the double integral on the right hand side vanishes at $s = L$. We arrive at

$$C = - \int_0^L \frac{ds'}{\phi(s')^2} \left(\int_0^{s'} ds'' \bar{x}(s'') \phi(s'')^2 \right) \div \int_0^L \frac{ds'}{\phi(s')^2} \quad (44)$$

for the first integration constant. Finally, we note that the slopes are continuous, $F'(L) = F'(0)$, since the integral of \bar{x} over the graph is zero by definition.

Similar remarks hold for the G functions. For example, for G in the x-direction, we find

$$G(s) = G(0) + \frac{2m}{\hbar^2} \int_0^s \frac{ds'}{\phi(s')^2} \times \left(\int_0^{s'} ds'' [\bar{x}(s'') F(s'') - \langle 0 | \bar{x} F | 0 \rangle] \phi(s'')^2 + D \right) \quad (45)$$

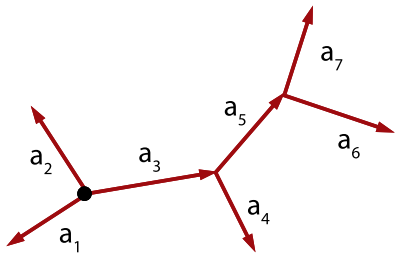


FIG. 7. Three prong graph with seven edges.

where the first integration constant is given by

$$D = - \int_0^L \frac{ds'}{\phi(s')^2} \quad (46)$$

$$\times \left(\int_0^{s'} ds'' [\bar{x}(s'')F(s'') - \langle 0|xF|0\rangle] \phi(s'')^2 \right)$$

$$\div \int_0^L \frac{ds'}{\phi(s')^2}$$

Fig 6 shows the two F functions and for G for the loop graph. It is clear that the boundary conditions caused the functions to assume periodic behavior.

D. Multiple star graph

We can extend the general algorithm to more complicated structures, such as the three prong graph having seven edges (a star at each end, and a star connecting these), shown in the left panel of Figure 7. For convenience, we can put the origin at the first star vertex, where edges a_1, a_2, a_3 are joined. Using the algorithm in Eqn 4, we need to find seven first constants of integration, $C_i, i = 1 - 7$. These are given by

$$C_1 = -\langle \bar{x}_1 \rangle$$

$$C_2 = -\langle \bar{x}_2 \rangle$$

$$C_3 = \langle \bar{x}_1 \rangle + \langle \bar{x}_2 \rangle$$

$$C_4 = -\langle \bar{x}_4 \rangle \quad (47)$$

$$C_5 = \langle \bar{x}_1 \rangle + \langle \bar{x}_2 \rangle + \langle \bar{x}_3 \rangle + \langle \bar{x}_4 \rangle$$

$$C_6 = -\langle \bar{x}_6 \rangle$$

$$C_7 = -\langle \bar{x}_7 \rangle \quad (48)$$

Note that we could have used the algorithm to rewrite C_6 as

$$C_6 = \langle \bar{x}_1 \rangle + \langle \bar{x}_2 \rangle + \langle \bar{x}_3 \rangle + \langle \bar{x}_4 \rangle + \langle \bar{x}_5 \rangle + \langle \bar{x}_7 \rangle \quad (49)$$

by Eqn 41.

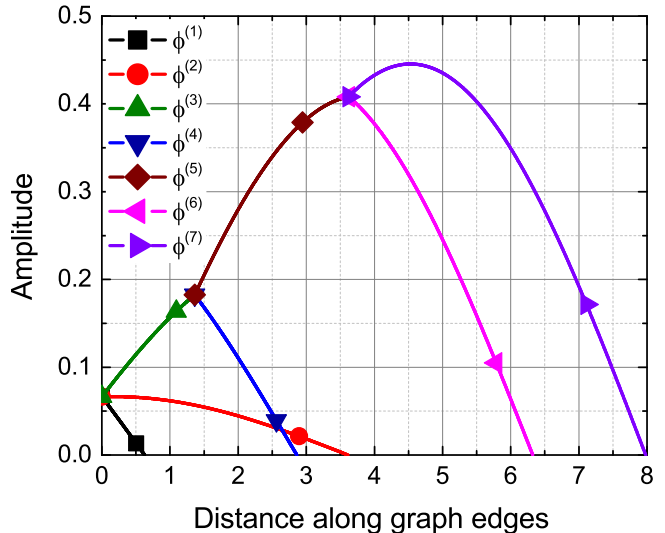


FIG. 8. Edge functions on three prong graph. The x-axis denotes distance from the origin (black dot) in Fig 5. The three vertices of this graph are shown as the intersection points of the edge functions. Continuity of the edge functions and conservation of their derivatives at each vertex are evident in the Figure.

Figure 8 shows the edge functions along the graph and illustrates their continuity and the conservation of flux. The edge lengths a_1 to a_7 are 0.63, 3.61, 1.36, 1.50, 2.26, 2.70, and 4.36, in arbitrary units, and their respective angles, in degrees, are 180, 60, 0, 60, 0, 36, and 0. Edges 1,2,4,6,7 terminate at an infinite potential wall, and the edge functions vanish there, as may be seen in the Figure.

Figure 9 shows that the SOS and DL results are identical using this formalism. The DL calculations executed ten times faster than using 20 modes in the SOS calculation. Moreover, the solution of the SOS calculation required careful computation of the amplitudes due to degeneracies in the graph. As graphs get larger, degeneracies become very difficult to compute, and the SOS method is impractical. The DL method does not require any information other than the ground state, which is nondegenerate.

Figures 10 and 11 show the F_i function along the x and y directions, respectively. The figures show that the computation has produced edge DL functions that are continuous and have conserved slope at their vertices.

V. CONCLUSIONS

The computation of the optical nonlinearities of quasi-dimensional systems, modeled by quantum graphs, has been adapted from the sum over states (SOS) to the Dalgarno-Lewis (DL) method and resulted in an execu-

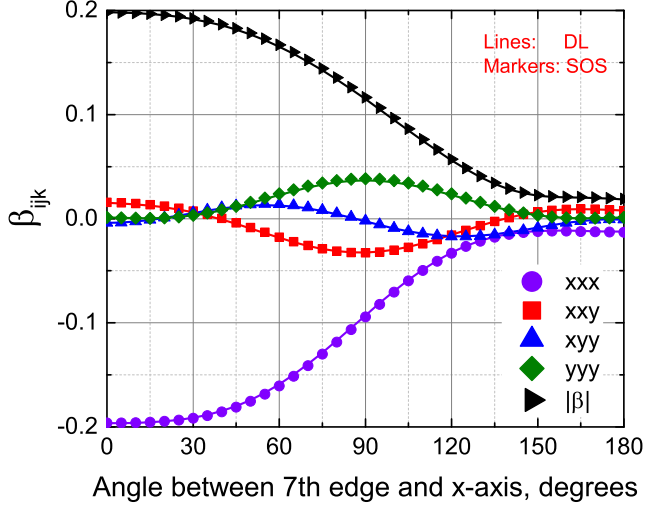


FIG. 9. First hyperpolarizability tensors, computed by DL (solid lines) and SOS (open lines) for the seven-edge graph described in the text. Both methods agree to under a few hundreds of a percent. The SOS calculation used 20 modes and executed ten times more slowly than the DL calculation.

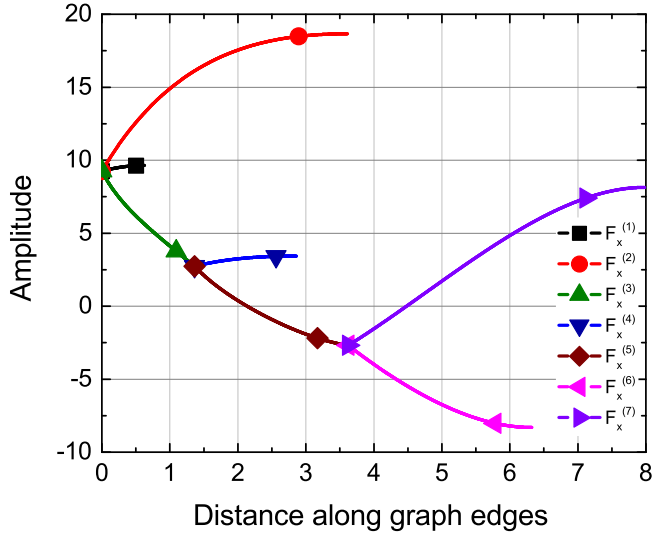


FIG. 10. $F_x^{(p)}$ functions for all graph edges using the same ordering scheme as used in Fig 8 for the edge functions. Note that the DL edge functions are continuous at the vertices, and their derivatives are conserved at the vertices.

tion time speedup of anywhere from a factor of 10 – 50 for a simple star graph. For large-scale Monte Carlo simulations normally taking hours with the SOS, the computation time is reduced to well under half an hour and often requires only a few minutes. SOS requires solving the quantum graph for all of its eigenfunctions and energies, whereas DL requires only knowledge of the ground state and, for intrinsic nonlinearities, the first two energy levels. A quantum graph with many edges has an exceed-

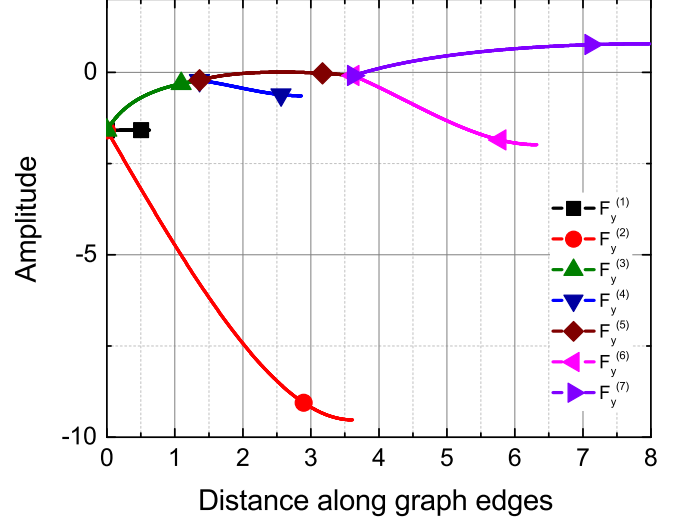


FIG. 11. $F_y^{(p)}$ functions for all graph edges using the same ordering scheme as used in Fig 8 for the edge functions. Note that the DL edge functions are continuous at the vertices, and their derivatives are conserved at the vertices.

ingly complex secular equation whose M roots must be found for an SOS over M states. Often, the roots are so closely spaced that numerical solutions are inaccurate, and it is impossible, a priori, to even know which roots are degenerate, let alone what the degree of degeneracy is. Subspaces of eigenfunctions with degenerate states must be diagonalized. The time to sum over states for β scales as M^2 , while for γ , it scales as M^3 . The adaptation of the DL method for quantum graphs provides a fast, reliable way for researchers to solve quantum graph models that would otherwise be nearly intractable.

Another benefit of the DL method is that it requires only the ground state of the system. This implies that one can, in principle, attempt to model structures with large response by testing various models of charge distribution in the ground state of a molecule. In a real system, the Hamiltonian determines the exact eigenstates and spectra, and for a given set of boundary conditions, the ground state would be unique. For modeling a system, one could mock up a ground state based upon intuition about how the charge is distributed in a test molecule, and then compute β and γ using the DL method. The test molecule's actual Hamiltonian might not produce a ground state that exactly resembles the mocked up version, but the result should be meaningful.

The DL method has been solved for the dispersive case and is presented in a paper in this special issue. The extension of the DL method for graphs to include dispersion is identical to the presentation here, except that the DL functions take a different form that depends on the optical frequencies and the linewidths.

VI. ACKNOWLEDGEMENTS

SMM and MGK thank the National Science Foundation (ECCS-1128076) for generously supporting this work.

-
- [1] S. Shafei, R. Lytel, and M. G. Kuzyk, “Geometry-controlled nonlinear optical response of quantum graphs,” *J. Opt. Soc. Am. B* **29**, 3419–3428 (2012).
- [2] R. Lytel, S. Shafei, J. H. Smith, and M. G. Kuzyk, “Influence of geometry and topology of quantum graphs on their nonlinear optical properties,” *Phys. Rev. A* **87**, 043824 (2013).
- [3] R. Lytel and M. G. Kuzyk, “Dressed quantum graphs with optical nonlinearities approaching the fundamental limit,” *Journal of Nonlinear Optical Physics & Materials* **22** (2013).
- [4] R. Lytel, S. Shafei, and M. G. Kuzyk, “Optimum topology of quasi-one-dimensional nonlinear optical quantum systems,” *Journal of Nonlinear Optical Physics & Materials* **23**, 1450025 (2014).
- [5] R. Lytel, S. M. Mossman, and M. G. Kuzyk, “Optimization of eigenstates and spectra for quasi-linear nonlinear optical systems,” *Journal of Nonlinear Optical Physics & Materials* **24**, 1550018 (2015).
- [6] R. Lytel, “Physics of the fundamental limits of nonlinear optics: A theoretical perspective,” *ArXiv e-prints* (2016).
- [7] L. Pauling, “The diamagnetic anisotropy of aromatic molecules,” *J. Chem. Phys.* **4**, 673 (1936).
- [8] H. Kuhn, “Free Electron Model for Absorption Spectra of Organic Dyes,” *J. Chem. Phys.* **16**, 840–841 (1948).
- [9] K. Ruedenberg and C. W. Scherr, “Free-electron network model for conjugated systems. i. theory,” *The Journal of Chemical Physics* **21**, 1565–1581 (1953).
- [10] C. W. Scherr, “Free-electron network model for conjugated systems. ii. numerical calculations,” *The Journal of Chemical Physics* **21**, 1582–1596 (1953).
- [11] J. R. Platt, “Free-electron network model for conjugated systems. iii. a demonstration model showing bond order and “free valence” in conjugated hydrocarbons,” *The Journal of Chemical Physics* **21**, 1597–1600 (1953).
- [12] D. Kowal, U. Sivan, O. Entin-Wohlman, and Y. Imry, “Transmission through multiply-connected wire systems,” *Physical Review B* **42**, 9009 (1990).
- [13] C. Flesia, R. Johnston, and H. Kunz, “Strong localization of classical waves: a numerical study,” *EPL (Europhysics Letters)* **3**, 497 (1987).
- [14] E. Ivchenko and A. Kiselev, “Electron g factor in quantum wires and quantum dots,” *Journal of Experimental and Theoretical Physics Letters* **67**, 43–47 (1998).
- [15] J. Sánchez-Gil, V. Freilikher, I. Yurkevich, and A. Maradudin, “Coexistence of ballistic transport, diffusion, and localization in surface disordered waveguides,” *Physical review letters* **80**, 948 (1998).
- [16] Y. Avishai and J. Luck, “Quantum percolation and ballistic conductance on a lattice of wires,” *Physical Review B* **45**, 1074 (1992).
- [17] C. Amovilli, F. E. Leys, and N. H. March, “Electronic energy spectrum of two-dimensional solids and a chain of c atoms from a quantum network model,” *Journal of mathematical chemistry* **36**, 93–112 (2004).
- [18] F. E. Leys, C. Amovilli, and N. H. March, “Topology, connectivity, and electronic structure of c and b cages and the corresponding nanotubes,” *Journal of chemical information and computer sciences* **44**, 122–135 (2004).
- [19] P. Kuchment and O. Post, “On the spectra of carbon nano-structures,” *Communications in Mathematical Physics* **275**, 805–826 (2007).
- [20] T. Kottos and U. Smilansky, “Quantum chaos on graphs,” *Phys. Rev. Lett.* **79**, 4794–4797 (1997).
- [21] T. Kottos and U. Smilansky, “Periodic orbit theory and spectral statistics for quantum graphs,” *Ann. Phys.* **274**, 76–124 (1999).
- [22] T. Kottos and U. Smilansky, “Chaotic scattering on graphs,” *Physical review letters* **85**, 968 (2000).
- [23] R. Blümel, Y. Dabaghian, and R. Jensen, “One-dimensional quantum chaos: explicitly solvable cases,” *JETP Lett* **74**, 258 (2001).
- [24] B. J. Orr and J. F. Ward, “Perturbation Theory of the Non-Linear Optical Polarization of an Isolated System,” *Molec. Phys.* **20**, 513–526 (1971).
- [25] R. Lytel, S. Mossman, and M. Kuzyk, “Phase disruption as a new design paradigm for optimizing the nonlinear-optical response,” *Optics Letters* **40**, 4735–4738 (2015).
- [26] A. Dalgarno and J. T. Lewis, “The exact calculation of long-range forces between atoms by perturbation theory,” *Proc. R. Soc. London Ser. A* **233**, 70–74 (1955).
- [27] S. Mossman, R. Lytel, and M. G. Kuzyk, “Dalgarno-lewis perturbation theory for nonlinear optics,” *arXiv preprint arXiv:1512.05824* (2015).
- [28] M. G. Kuzyk, “Physical Limits on Electronic Nonlinear Molecular Susceptibilities,” *Phys. Rev. Lett.* **85**, 1218 (2000).
- [29] R. Lytel, S. Shafei, and M. G. Kuzyk, “Scaling and universality in nonlinear optical quantum graphs containing star motifs,” *arXiv preprint arXiv:1305.4334* (2013).
- [30] J. Jerphagnon, D. Chemla, and R. Bonneville, “The description of the physical properties of condensed matter using irreducible tensors,” *Adv. Phys.* **27**, 609–650 (1978).
- [31] W. Thomas, “Über die zahl der dispersionselektronen, die einem stationären zustande zugeordnet sind.(vorläufige mitteilung),” *Naturwissenschaften* **13**, 627–627 (1925).
- [32] F. Reiche and u. W. Thomas, “Über die zahl der dispersionselektronen, die einem stationären zustande zugeordnet sind,” *Z. Physik* **34**, 879 (1925).
- [33] W. Kuhn, “Über die gesamtstarke der von einem zustande ausgehenden absorptionslinien,” *Zeitschrift für*

- Physik A: Hadrons and Nuclei **33**, 408–412 (1925).
- [34] H. A. Mavromatis, “The dalgarno-lewis summation technique: Some comments and examples,” *Am. J. Phys.* **59**, 738–744 (1991).
- [35] S. M. Harris, “Cranking model calculation of the moment of inertia using the method of dalgarno and lewis,” *American Journal of Physics* **45**, 373–375 (1977).
- [36] M. Maize, M. Antonacci, and F. Marsiglio, “The static electric polarizability of a particle bound by a finite potential well,” *American Journal of Physics* **79**, 222–225 (2011).
- [37] L. I. Schiff, *Quantum Mechanics*, International Pure and Applied Physics Series (McGraw-Hill, New York, 1968), 3rd ed.
- [38] S. Shafei and M. G. Kuzyk, “The effect of extreme confinement on the nonlinear-optical response of quantum wires,” *J. Nonl. Opt. Phys. Mat.* **20**, 427–441 (2011).
- [39] R. Lytel, S. Shafei, and M. G. Kuzyk, “Nonlinear optics of quantum graphs,” in “*Proc. SPIE 8474*,” (2012), pp. 84740O–84740O–9.